Journal of
Proteomics & Bioinformatics

Gridley et al., J Proteomics Bioinform 2012, 5:10
DOI: 10.4172/jpb.1000246

Research Article Open Access

Effects of Space Flight on the Expression of Liver Proteins in the Mouse

Daila S. Gridley[1,2], Michael J. Pecaut[1,2], Lora M. Green[1], E. Clifford Herrmann[2], Brandon Bianski[1], James M. Slater[1], Louis S. Stodieck[4], Virginia L. Ferguson[4] and Lawrence B. Sandberg[2,3]*

[1]*Department of Radiation Medicine, Loma Linda University and Medical Center, Loma Linda, CA 92354, USA*
[2]*Department of Basic Sciences, Loma Linda University and Medical Center, Loma Linda, CA 92354, USA*
[3]*Department of Rheumatology, Pathology and Human Anatomy, Loma Linda University and Medical Center, Loma Linda, CA 92354, USA*
[4]*Department of Aerospace Engineering, Bioserve Space Technologies, University of Colorado, Boulder, CO 80309, USA*

Abstract

Raw data derived from mass spectroscopic (MS) analyses of formalin-fixed paraffin-embedded (FFPE) tissue sections of the essential metabolic organ, liver, allocated by the provider (Amgen) from mice subjected to 13 days of microgravity on NASA Flight STS-118 were analyzed by two different search engines, using shotgun proteomics. With the eight statistically significant readouts in hand, Ingenuity Pathway Analysis (IPA) was employed to visualize probable biologic pathway relationships among proteins that might be associated with alterations in liver biochemistry due to space flight. Most noteworthy was the finding of up-regulation of the first urea cycle enzyme carbamoyl-phosphate synthetase, consistent with increased amino acid catabolism resulting from gravitational changes, and/or other stress associated with missions in space. Down-regulation of fructose-bisphosphate aldolase B, regucalcin, ribonuclease UK114, alpha enolase, glycine N-methyltransferase and S-adenosyl methionine synthetase isoform type-1 was observed. 60 kDa heat shock protein was elevated.

Keywords: Liver detoxification; Microgravity; Rodent; Tandem mass spectrometry; Urea cycle

Introduction

Spaceflight has been shown to affect a number of mammalian body systems. This report provides experimental data on liver proteins of mice that were part of the Commercial Biomedical Test Module-2 flown on the space shuttle Endeavour (STS-118), a 13-day mission to the International Space Station in August, 2007. Several studies on these mice have now been published [1-7]. In earlier studies on humans, loss of Lean Body Mass (LBM), fat and water, as well as loss of strength and changes in plasma protein and amino acid levels were reported. An increase in urinary interleukin-6 (IL-6) on the first day of flight in the Columbia space shuttle indicated an acute-phase response from the liver [8]. Using a ^{15}N-glycine tracer technique to study protein turnover in four Russian cosmonauts and two U.S. astronauts residing long term aboard the MIR orbital station, investigators found a nearly 50% decrease in protein synthesis [9]. In a review of the literature, Stein and Wade [10] noted that the shift towards increased activity of glycolytic enzymes associated with muscle atrophy, a major concern during spaceflight, is accompanied by increased gluconeogenesis in the liver. Leach et al. [11] showed that there are increased levels of 3-methyl histidine, creatinine and sarcosine due to muscle breakdown, and decreased levels of plasma albumin and transferrin inferring inadequate dietary protein intake on the early Soviet and Skylab missions. The protein depletion seen in astronauts upon landing after missions is followed by a post-flight anabolic phase so that muscles regain normal protein levels, a process that apparently can affect protein status in other body compartments [12]. These above studies, done with hippuric acid (^{15}N glycine) administration and plasma sampling showed that the fractional synthetic rates of fibrinogen, complement C-3, ceruloplasmin, and haptoglobin were low on day 6 after landing compared to pre-flight measurements. These findings were consistent with limited amino acid availability due to substrate competition between muscles and other tissues.

The hypothesis of this present study was that there will be distinct changes in the profile of major liver proteins of the mouse that are introduced by conditions associated with spaceflight. This profile may occur in humans, as well after a mission in space.

Materials and Methods

Animals and liver sample collection

C57BL/6NTac female mice (n=10; Taconic Farms, Inc., Germantown, NY) were shipped at about 7 weeks of age to the National Aeronautics and Space Administration (NASA) Space Life Sciences Laboratory (SLSL) at the Kennedy Space Center. For both flight (FLT) and ground control (GRD) mice, similarity of housing conditions in animal enclosure modules (AEM) and acclimatization procedures prior to take off have been described [1]. The FLT mice flew onboard the Space Shuttle Endeavour (STS-118) for 13 days. By using telemetry from the shuttle, the AEM-housed GRD were exposed to environmental conditions comparable to FLT animals (i.e. temperature, humidity, CO_2) on a 48-h delay. The FLT and GRD mice housed in the AEMs were equipped with solid food bars and a water dispenser so that nourishment was available continually even after landing. Within 3-6 h after landing of the space shuttle, FLT and GRD mice were evaluated for muscle strength and scanned with nuclear magnetic resonance imaging to assess lean and fat mass composition (performed by Amgen investigators). Mice were then euthanized with 100% CO_2. The NASA, Amgen, Inc., Loma Linda University and University of Colorado Institutional Animal Care and Use Committees

***Corresponding author:** Lawrence B. Sandberg, Department of Basic Sciences, Loma Linda University, MT 231, 11085 Campus Street, Loma Linda, California 92354, USA, Tel: 909-558-4527; Fax: 909-558-4887; E-mail: lsandberg@llu.edu

Received October 05, 2012; **Accepted** October 27, 2012; **Published** October 30, 2012

Citation: Gridley DS, Pecaut MJ, Green LM, Herrmann EC, Bianski B, et al. (2012) Effects of Space Flight on the Expression of Liver Proteins in the Mouse. J Proteomics Bioinform 5: 256-261. doi:10.4172/jpb.1000246

approved this study. A Material Transfer Agreement was also obtained for the transfer of mouse tissues. Liver tissues were alloted to the Loma Linda NASA Laboratory by Amgen.

Protein analysis

FFPE tissue blocks were prepared from the livers harvested from FLT and GRD mice (5 in each group, 10 animals total). The latter served as the basis for comparisons in this study. Sections were cut at 10 μm thickness and de-paraffinized, but not cover-slipped. Serial sections for protein sampling remained unstained and were stored briefly in water. Areas of the FLT and GRD liver sections selected for uniformity were removed from the slides with a 3 mm punch. These punched tissue samples, each containing approximately 30,000 cells, were placed in 20 μL of Expression Pathology digestion buffer (www.expressionpathology.com). (Expression Pathology Inc. Rockville, MD). The Expression Pathology protocol for digest preparation and analysis was followed precisely for all the samples. This consisted of first heating the punched tissue samples in the proprietary digestion buffer at 95°C for 1 h. This was followed by digestion with sequencing grade trypsin (www.promega.com) (Promega Corp. Madison WI), overnight at 37°C. Small aliquots were analyzed for protein content using a Micro BCA Protein Assay Kit (www.piercenet.com) (Thermo Fisher Scientific, Rockford, IL), prior to subjecting the remaining digest to dithiothreitol reduction. Peptide samples 1.5 μg by protein assay from each digest were then evaluated by LC/MS/MS on a Thermo-Electron LCQ Deca XP mass spectrometer (www.thermo.com) (Thermo Fisher Scientific), using nano-electrospray equipment produced by New Objective, Woburn, MA (www.newobjective.com). This consisted of reverse-phase collection of peptides on a 2 cm x 75 μm capture column followed by separation of peptides on a 10 cm x 75 μm vented analytical column [13], using Micro Magic RP-18AQ resin (www.michrom.com) (Michrom Bioresources, Inc., Auburn, CA). MS analyses were accomplished with a 5-part protocol cycle that consisted of one full MS survey scan (from 400 to 1700 m/z), followed by acquisition of collisional-induced dissociation tandem mass spectra of the four most intense ions in the survey scan. The nanoflow solvent gradient (linear 2-60% acetonitrile) extended over 3 h, using solvent B (95% acetonitrile with 0.1% formic acid) developed against solvent A (2% acetonitrile with 0.1% formic acid), at a flow rate of 250-300 nL/min. Samples were run as groups of five followed by water blank, preceeded and followed by a Michrom BSA trypsin-digested control followed by a water blank. Minimal carryover was detected in the water blanks.

Data analysis

Runs were first evaluated by the Thermo Bioworks software generating .dta files, then Perl .mgf files (www.perl.com) for evaluation by the Mascot search engine (www.matrixscience.com), using an International Protein Index (IPI) mouse FASTA library (www.ebi.ac.uk/IPI), modified to a concatenated format so as to detect false discoveries. These results were then moved into Scaffold (version 3.3.3) (www.proteomesoftware.com). Merged resultant files from Mascot and X!-Tandem (www.thegpm.com) within Scaffold gave a final readout of the analysis, using the spectral quantitative value display option with filter settings of: Min Protein 95%, Min # Peptides 2, min Peptide 95%. This gave 67 proteins identified for this dataset. The aim to obtain highly reliable but not necessarily comprehensive quantitative data was attained in positive and negative format by expression as $\log_2$ fold changes (FLT/GRD). Thus IPA, which utilizes fold change data as well as P-values for reliability, gave good pathway analyses with this format. By combining FLT and GRD data within Scaffold and entering each analysis as a separate biosample, a T-test analysis was generated between the FLT and GRD groups, and also a $\log_2$ fold change for each from FLT AVG / GRD AVG calculations was created. The Quantitative Value display option with Total Ion Current (TIC) was chosen as the quantitative method.

Statistical and pathway analyses

For this type of data, the T-test method of analysis has been shown to be the best [14]. These two groups (FLT and GRD) of data were then analyzed through the use of Ingenuity Pathways Analysis (IPA) (Ingenuity Systems, Redwood City, CA) (www.ingenuity.com) to generate significant pathway networks, and for comparison with canonical pathway networks within the IPA databases. Data was thus entered into IPA using the IPI accession numbers, the P-values and $\log_2$ fold change values, the latter allowed demonstration of positive (up-regulated) and negative (down-regulated) values for the flight group within IPA (Table 1). The entire contents of the Scaffold analysis dataset, table 1 (67 proteins) was fed into IPA because even proteins of lower significance (P-value>0.050) have an advantageous influence on the outcome of the pathway analysis (Figure 1).

Results and Discussion

In our present MS study comparing FLT versus GRD mice, measurement of statistically significant ($P<0.05$) changes of eight proteins was achieved in a specific mouse organ, the liver, via an innovative methodology that allows analysis of FFPE tissue for total tissue protein composition. The Expression Pathology reagents and procedure provided a simple method for obtaining these data from FFPE tissues (without this statistical data, no one could have accomplished this study). Scaffold yielded a spectral quantitative value and total ion current for each peptide identified within each analysis of the MS/MS data. Of the 8 proteins, only carbamoyl-phosphate synthetase and 60 kDa heat shock protein, a chaperonin, gave significant positive $\log_2$ fold change values. Carbamoyl-phosphate synthetase was the protein present in highest concentration. This enzyme provides the entry point of ammonia into the urea cycle, and is found primarily in the liver [15]. The urea cycle is the major mechanism for ridding the organism of catabolic ammonia. The other enzymes of the urea cycle (ornithine carbamoyltransferase, argininosuccinate synthetase, argininosuccinate lyase and arginase-1) were also apparent in the MS spectra, but their levels were not significantly altered between FLT mice and GRD controls. These are also present in table 1. Their inter-relationship is shown in figure 2. Because it is up-regulated, carbamoyl-phosphate synthetase appears to be the major urea cycle regulatory enzyme in these mice.

Ammonia in excess of that transformed into urea is toxic to cells via the glutamate dehydrogenase (GDH) catalyzed reaction, even though nontoxic glutamate is produced. The toxicity is due to the concomitant depletion of alpha keto glutarate, by the GDH-catalyzed reaction and consequently, the other Krebs cycle intermediates [15]. Thus, a metabolic result of detoxifying excess ammonia by GDH activity lowers the amount of oxaloacetate, the substrate required for entry of acetyl coenzyme A into the Krebs cycle; with the result that energy metabolism is inhibited. Up-regulation of GDH is indicated in FLT liver samples, although not statistically significant (Table 1). Even

SYMBOL	Identified Proteins (67)	Accession #	Mol Wt	P-Value	FC	LOG2_FC	FLT AVG	FLT SDEVA	GRD AVG	GRD SDEVA
RGN	Regucalcin	IPI00133456	33 kDa	0.0021	0.415	-1.27	1.17E+08	7.16E+07	2.82E+08	4.15E+07
ALDOB	Fructose-bisphosphate aldolase B	IPI00127206	40 kDa	0.0033	0.483	-1.051	2.42E+08	6.57E+07	5.01E+08	1.24E+08
ENO1	Alpha-enolase	IPI00462072	47 kDa	0.0039	0.259	-1.949	1.10E+07	1.01E+07	4.25E+07	1.43E+07
GNMT	Glycine N-methyltransferase	IPI00467066	33 kDa	0.007	0.327	-1.614	4.06E+07	4.33E+07	1.24E+08	2.88E+07
HRSP12	Ribonuclease UK114	IPI00130640	14 kDa	0.0082	0.262	-1.932	1.27E+07	1.72E+07	4.86E+07	1.53E+07
CPS1	Carbamoyl-phosphate synthase [ammonia], mitochondrial	IPI00111908	165 kDa	0.015	1.202	0.265	3.31E+09	1.80E+08	2.75E+09	3.63E+08
HSPD1	Isoform 1 of 60 kDa heat shock protein, mitochondrial	IPI00308885	61 kDa	0.043	2.564	1.358	2.95E+07	3.97E+06	1.15E+07	1.63E+07
MAT1A	S-adenosylmethionine synthetase isoform type-1	IPI00128518	44 kDa	0.048	0.62	-0.69	8.22E+07	2.72E+07	1.33E+08	3.99E+07
FAS	Fatty acid synthase	IPI00113223	272 kDa	0.052	0.115	-3.116	1.00E+06	0.00E+00	8.67E+06	7.60E+06
ATP5B	ATP synthase subunit beta, mitochondrial	IPI00468481	56 kDa	0.056	1.419	0.504	2.07E+08	2.48E+07	1.46E+08	5.60E+07
SDH	Sarcosine dehydrogenase, mitochondrial	IPI00136213	102 kDa	0.058	0.246	-2.025	3.94E+06	6.57E+06	1.60E+07	1.04E+07
HMGCS1	Hydroxymethylglutaryl-CoA synthase, mitochondrial	IPI00420718	57 kDa	0.08	2.7	1.433	1.03E+08	7.08E+07	3.80E+07	1.35E+07
ATP5A	ATP synthase subunit alpha, mitochondrial	IPI00130280	60 kDa	0.096	0.784	-0.352	6.18E+07	9.00E+06	7.88E+07	1.81E+07
CPN10	CPN10-like protein	IPI00120045	11 kDa	0.097	18.121	4.18	1.81E+07	2.06E+07	1.00E+06	0.00E+00
MSDH	Methylmalonate-semialdehyde dehydrogenase, mitochondrial	IPI00461964	58 kDa	0.11	3.401	1.766	9.66E+06	7.61E+06	2.84E+06	4.12E+06
PRDX1	Peroxiredoxin-1	IPI00121788	22 kDa	0.13	0.404	-1.307	2.24E+07	3.09E+07	5.54E+07	3.17E+07
GLUD1	Glutamate dehydrogenase 1, mitochondrial	IPI00114209	61 kDa	0.16	1.264	0.338	1.60E+08	3.25E+07	1.26E+08	3.47E+07
KRT8	Keratin, type II cytoskeletal 8	IPI00322209	55 kDa	0.17	4.352	2.122	4.35E+06	4.75E+06	1.00E+06	0.00E+00
	Putative uncharacterized protein	IPI00322209	55 kDa	0.17	4.352	2.122	4.35E+06	4.75E+06	1.00E+06	0.00E+00
BHMT	Betaine--homocysteine S-methyltransferase 1	IPI00130950	45 kDa	0.2	1.661	0.732	1.47E+08	3.21E+07	8.88E+07	8.90E+07
	37 kDa protein	IPI00123176	37 kDa	0.24	0.515	-0.958	4.72E+07	4.21E+07	9.17E+07	6.56E+07
H2BA	Histone H2B type 1-A	IPI00111957	14 kDa	0.25	3.592	1.845	4.48E+07	5.35E+07	1.25E+07	2.12E+07
PK	Pyruvate kinase isozymes R/L	IPI00133605	62 kDa	0.31	0.283	-1.82	1.00E+06	0.00E+00	3.53E+06	5.66E+06
ASS	Argininosuccinate synthase	IPI00134746	47 kDa	0.33	1.144	0.194	3.15E+08	5.31E+07	2.75E+08	6.67E+07
SDH	Sorbitol dehydrogenase	IPI00753038	38 kDa	0.33	2.687	1.426	1.26E+07	1.62E+07	4.70E+06	6.16E+06
KRT18	Keratin, type I cytoskeletal 18	IPI00311493	48 kDa	0.35	6.202	2.633	6.20E+06	1.16E+07	1.00E+06	0.00E+00
DMGDH	Dimethylglycine dehydrogenase, mitochondrial	IPI00120123	97 kDa	0.35	0.386	-1.373	1.00E+06	0.00E+00	2.59E+06	3.55E+06
ALB	Serum albumin	IPI00131695	69 kDa	0.37	0.511	-0.97	3.11E+07	2.89E+07	6.09E+07	6.38E+07
	Putative uncharacterized protein	IPI00652436	42 kDa	0.41	0.885	-0.176	3.14E+08	7.84E+07	3.55E+08	6.97E+07
GSTM1	Glutathione S-transferase Mu 1	IPI00230212	26 kDa	0.41	0.769	-0.379	1.44E+08	5.13E+07	1.87E+08	9.85E+07
eEF1a1	Elongation factor 1-alpha 1	IPI00307837	50 kDa	0.42	1.35	0.433	1.08E+08	2.82E+07	7.97E+07	6.83E+07
	Putative uncharacterized protein	IPI00122815	57 kDa	0.42	1.779	0.831	3.18E+06	3.01E+06	1.78E+06	1.75E+06
HPPD	4-hydroxyphenylpyruvate dioxygenase	IPI00554931	45 kDa	0.44	0.692	-0.53	3.53E+07	2.67E+07	5.09E+07	3.42E+07
	Putative uncharacterized protein	IPI00331692	32 kDa	0.44	3.2	1.678	4.86E+06	8.63E+06	1.52E+06	1.16E+06
CA3	Carbonic anhydrase 3	IPI00221890	29 kDa	0.45	2.076	1.054	3.38E+07	4.41E+07	1.63E+07	1.91E+07
	Putative uncharacterized protein	IPI00114710	130 kDa	0.46	1.768	0.822	1.15E+07	1.20E+07	6.52E+06	7.56E+06
AST	Aspartate aminotransferase, mitochondrial	IPI00117312	47 kDa	0.47	0.728	-0.457	2.93E+07	1.63E+07	4.02E+07	2.73E+07
SOD	Superoxide dismutase [Cu-Zn]	IPI00130589	16 kDa	0.48	0.694	-0.526	1.89E+07	1.44E+07	2.72E+07	2.09E+07
HSP84b	MCG18238	IPI00229080	83 kDa	0.49	0.785	-0.349	2.11E+07	1.63E+07	2.69E+07	8.36E+06
AHCY	Adenosylhomocysteinase	IPI00230440	48 kDa	0.5	0.804	-0.315	9.56E+07	5.04E+07	1.19E+08	5.29E+07
ETFA	Electron transfer flavoprotein subunit alpha, mitochondrial	IPI00116753	35 kDa	0.51	1.487	0.573	1.85E+07	1.71E+07	1.24E+07	9.28E+06
ACAT	3-ketoacyl-CoA thiolase A, peroxisomal	IPI00121833	44 kDa	0.51	0.417	-1.263	1.23E+06	3.27E+05	2.96E+06	4.38E+06

	trypsinogen 7	IPI00131674	26 kDa	0.53	0.777	-0.363	8.50E+07	7.93E+07	1.09E+08	2.52E+07
H2A	Histone H2A.J	IPI00153400	14 kDa	0.53	0.776	-0.366	5.41E+07	3.35E+07	6.97E+07	4.17E+07
ETFB	Electron transfer flavoprotein subunit beta	IPI00121440	28 kDa	0.53	2.031	1.022	1.31E+07	2.02E+07	6.45E+06	9.28E+06
H4	similar to histone H4	IPI00623776	17 kDa	0.55	0.829	-0.271	1.03E+08	6.60E+07	1.24E+08	3.63E+07
	protease, serine, 1	IPI00130391	26 kDa	0.56	1.424	0.51	3.38E+08	2.26E+08	2.37E+08	2.94E+08
ECH1	Enoyl-Coenzyme A, hydratase	IPI00127276	78 kDa	0.56	0.746	-0.422	1.59E+06	1.32E+06	2.13E+06	1.56E+06
OTC	Ornithine carbamoyltransferase, mitochondrial	IPI00116603	40 kDa	0.57	0.715	-0.483	2.04E+07	1.97E+07	2.85E+07	2.32E+07
UO	Uricase	IPI00223367	35 kDa	0.59	0.599	-0.739	1.15E+07	1.05E+07	1.92E+07	2.79E+07
CYB5	Cytochrome b5	IPI00230113	15 kDa	0.59	0.549	-0.866	1.65E+07	2.69E+07	3.01E+07	4.70E+07
TPI(TIM)	Triosephosphate isomerase	IPI00467833	27 kDa	0.59	1.665	0.735	2.37E+06	3.06E+06	1.42E+06	9.46E+05
ADH	Alcohol dehydrogenase 1	IPI00221400	40 kDa	0.6	0.784	-0.352	7.08E+07	4.19E+07	9.04E+07	6.90E+07
ARG1	Arginase-1	IPI00117914	36 kDa	0.6	1.28	0.356	5.59E+07	3.62E+07	4.37E+07	3.49E+07
HBB	Beta-globin	IPI00831055	16 kDa	0.62	0.866	-0.207	2.89E+08	1.61E+08	3.34E+08	1.04E+08
TUBA1A	Tubulin alpha-1A chain	IPI00110753	50 kDa	0.62	0.648	-0.625	4.37E+06	4.69E+06	6.74E+06	8.50E+06
	Putative uncharacterized protein	IPI00110658	15 kDa	0.68	1.468	0.554	1.73E+08	2.80E+08	1.18E+08	4.56E+07
	Putative uncharacterized protein	IPI00653931	46 kDa	0.7	0.78	-0.358	2.29E+07	1.82E+07	2.94E+07	3.10E+07
	10-formyltetrahydrofolate dehydrogenase	IPI00153317	99 kDa	0.72	0.736	-0.442	1.86E+07	3.26E+07	2.53E+07	2.76E+07
HSPA8	Hspa8 protein	IPI00886297	69 kDa	0.72	0.825	-0.277	8.37E+06	8.99E+06	1.01E+07	6.50E+06
ACAT	3-ketoacyl-CoA thiolase, mitochondrial	IPI00226430	42 kDa	0.73	0.934	-0.099	2.12E+08	8.59E+07	2.27E+08	4.03E+07
ALDH	Aldehyde dehydrogenase, mitochondrial	IPI00111218	57 kDa	0.82	0.942	-0.086	1.36E+08	5.20E+07	1.44E+08	5.73E+07
ASL	Argininosuccinate lyase	IPI00314788	52 kDa	0.82	0.857	-0.223	3.54E+07	2.66E+07	4.13E+07	4.98E+07
PFN1	Profilin-1	IPI00224740	15 kDa	0.82	0.888	-0.172	1.36E+06	4.96E+05	1.53E+06	7.42E+05
CAT	Catalase	IPI00869393	60 kDa	0.88	1.043	0.061	1.05E+08	3.35E+07	1.01E+08	5.84E+07
FBP	Fructose-1,6-bisphosphatase 1	IPI00228630	37 kDa	0.93	0.921	-0.118	1.51E+07	1.86E+07	1.63E+07	2.10E+07
FABP	Fatty acid-binding protein, liver	IPI00120451	14 kDa	0.95	0.987	-0.019	3.70E+08	1.32E+08	3.75E+08	8.65E+07

Table 1: 67-protein dataset generated in Scaffold with windows set at high stringencies (95% for both minimum protein and peptide identification probabilities, with 2 unique peptides). Proteins are sorted with respect to P-Values. 8 proteins have values <0.05. Averages of TIC counts for each of the 5 FLT analyses and 5 GRD analyses are shown as well as standard deviations (SD FLT & SD GRD), fold changes (FC) and LOG2 FC. Fold changes were calculated from FLT/GRD ratios. For computational purposes, all zero values within Scaffold were reset to 1000000.

though an elevation of GDH may seem advantageous for ammonia detoxification, the downside would be decreased in the capacity for energy production from glucose metabolism. The data for carbamoyl phosphate synthetase and GDH strongly suggest a compensatory mechanism in the FLT mice to deal with an ammonia overload caused by excessive protein catabolism. Skeletal muscle is the largest active protein pool in the body, and is the major site of protein catabolism. It is reported that blood urea nitrogen levels double during the first month of spaceflight. In astronauts, a 6-day mission resulted in a 3.5 kg loss of LBM [8]. Glycine N-methyltransferase, a methyl group transferring enzyme which participates in detoxification chemistry in liver cells [16] is down-regulated (Table 1). Studies have shown an insulin c-peptide elevation in astronauts of the American Space Shuttle missions, as high as 40% above normal after 9 days of flight [8]. This might infer a hyper insulinemia in an attempt to increase cellular uptake of glucose or perhaps indicate an insulin resistance, both of which relate to an intracellular glucose deficit contributing to increased protein catabolism. In contrast with the data which indicate protein catabolism, Ferrando et al. [17] state that the primary adaptation to space flight is not an increase in protein breakdown, but rather the body's inability to maintain protein synthesis in skeletal muscle. They feel that the most apparent factor in the loss of LBM is reduced energy intake during spaceflight (25-30% on some spaceflights). The data suggest in agreement with Stein & Gaprindashvili [8], that insulin resistance may also be a factor. The down-regulated fructose-bisphosphate aldolase B levels were observed and are also consistent with this observation (Table 1). Insulin positively regulates fatty acid synthesis by increasing fatty acid synthase (FAS) mRNA transcription [18], but FAS as it appears in (Table 1) is markedly down-regulated. However, the P-value for FAS is below the significance cutoff of 0.050 in our study because the quality of the spectra as they appear in Scaffold is sub-optimal. Thus, our FAS data should be considered unreliable.

The smallness of this protein data set (67 proteins) may stem from the MS instrumentation that was available, but even though not complete, it represents the potential of utilizing FFPE tissue for conducting studies of this type and represents a beginning of understanding, of what takes place in the mammalian liver with weightlessness followed by stress of landing. Eight of the 67 proteins show statistical differences between FLT and GRD. Six were mapped by IPA. Some of these are linked to detoxification pathways within the liver (carbamoyl-phosphate synthetase, glycine N-methyltransferase, S-adenosylmethionine synthetase), and some to carbohydrate metabolism (fructose-bisphosphate aldolase B, alpha-enolase). 60 kDa heat shock protein was up-regulated, probably because of its

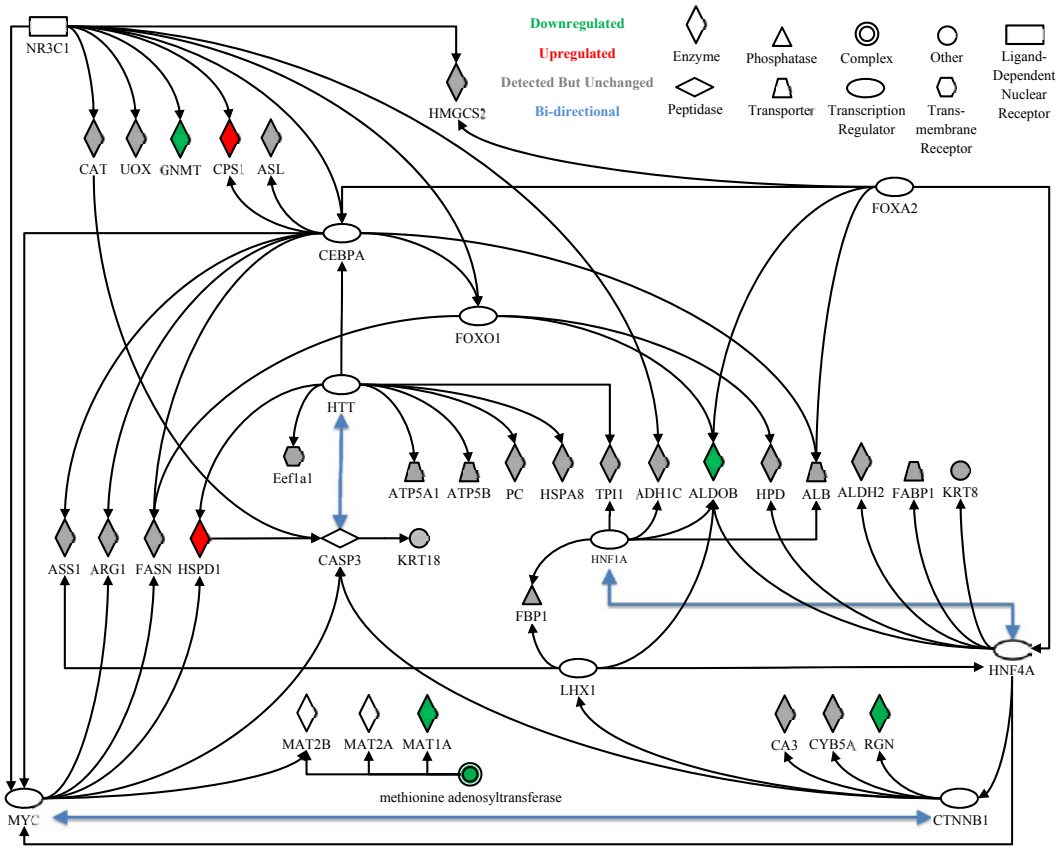

Figure 1: Through the use of the Ingenuity Pathway Analysis software and interactive website, we linked 6 of the 8 liver proteins, and their pathways, which we found to be significantly altered by spaceflight (Table 1). These are all enzymes (CSP1, ALDOB, HSPD1, GNMT, MAT1A and RGN); these proteins in red or green are up or down regulated respectively, at least 1.5 fold over GRD values (except for CPS1 which is 1.2). All of the end-product proteins except PC (pyruvate carboxylase) are represented in Table 1.

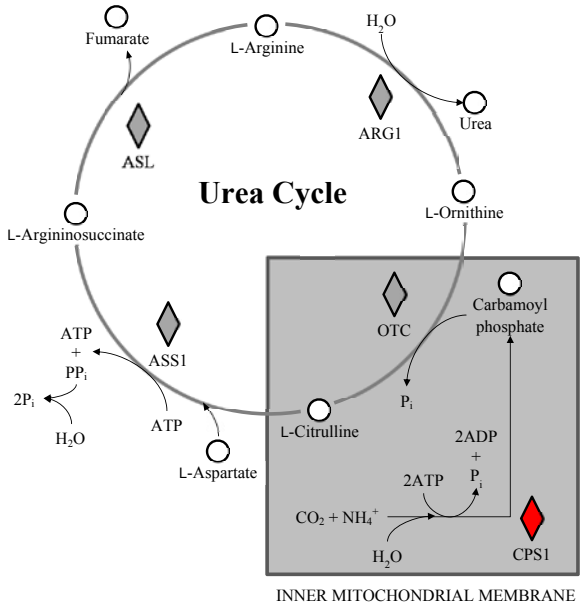

Figure 2: Enzymes of the urea cycle, all of which are identified in our dataset (Table 1). CPS1 = carbamoyl-phosphate synthetase, OTC = ornithine carbamoyltransferase, ASS1 = argininosuccinate synthetase, ASL = argininosuccinate lyase and ARG1 = arginase-1. Captions and colors are the same as in Figure 1. From Boyer (15).

relation to stress. Regucalcin was highly down-regulated possibly limiting osteoporosis, which is a major problem with space flight [19]. Overexpression of regucalcin has been shown to induce bone loss in rats [20]. Ribonuclease UK114, also known as heat-responsive protein 12 [21], was down-regulated possibly due to the stress of space flight as well.

Acknowledgments

The authors are grateful for Amgen, Inc., for sponsoring the flight investigation and generously providing the tissues required to conduct this study. In particular, we thank HQ Han and David Lacey, the principal investigators at Amgen. We also thank Ramona Bober and the rest of the staff at NASA Space Life Sciences Laboratory (SLSL) at the Kennedy Space Center for their support, and the students and technicians from the University of Colorado for assistance with tissue collection. Dr. Gregory A. Nelson and Tamaki Jones at Loma Linda University also assisted in various aspects of this study.

References

1. Baqai FP, Gridley DS, Slater JM, Luo-Owen X, Stodieck LS, et al. (2009) Effects of spaceflight on innate immune function and antioxidant gene expression. J Appl Physiol 106: 1935-1942.

2. Ortega MT, Pecaut MJ, Gridley DS, Stodieck LS, Ferguson V, et al. (2009) Shifts in bone marrow cell phenotypes caused by spaceflight. J Appl Physiol 106: 548-555.

3. Lebsack TW, Fa V, Woods CC, Gruener R, Manziello AM, et al. (2010) Microarray analysis of spaceflown murine thymus tissue reveals changes in gene expression regulating stress and glucocorticoid receptors. J Cell Biochem 110: 372-381.

4. Gridley DS, Slater JM, Luo-Owen X, Rizvi A, Chapes SK, et al. (2009)

Spaceflight effects on T lymphocyte distribution, function and gene expression. J Appl Physiol 106: 194-202.

5. Stevens L, Bastide B, Hedou J, Montel V, Dupont E, et al. (2008) Regulation of Muscle Plasticity by MLC2 Post-Translational Modifications After WISE Bedrest. Session 3: Muscle and metabolism physiology (18), Life in Space for Life on Earth.

6. Atiakshin DA, Bykov EG, Il'in EA, Pashkov AN (2009) Glycogen content in gerbil's liver following the spacecraft Foton-M3 mission. Aviakosm Ekolog Med 43: 18-22.

7. Baba T, Nishimura M, Kuwahara Y, Ueda N, Naitoh S, et al. (2008) Analysis of gene and protein expression of cytochrome P450 and stress-associated molecules in rat liver after spaceflight. Pathol Int 58: 589-595.

8. Stein TP, Gaprindashvili T (1994) Spaceflight and protein metabolism, with special reference to humans. Am J Clin Nutr 60: 806S-819S.

9. Stein TP, Larina IM, Leskiv MJ, Schluter MD (2000) Protein turnover during and after extended space flight. Aviakosm Ekolog Med 34: 12-16.

10. Stein TP, Wade CE (2005) Metabolic consequences of muscle disuse atrophy. J Nutr 135: 1824S-1828S.

11. Leach CS, Lane HW, Krauhs JM (1994) Short-term space flight on nitrogenous compounds, lipoproteins, and serum proteins. J Clin Pharmacol 34: 500-509.

12. Stein TP, Schluter MD (2006) Plasma protein synthesis after spaceflight. Aviat Space Environ Med 77: 745-748.

13. Licklider LJ, Thoreen CC, Peng J, Gygi SP (2002) Automation of nanoscale microcapillary liquid chromatography-tandem mass spectrometry with a vented column. Anal Chem 74: 3076-3083.

14. Zhang B, VerBerkmoes NC, Langston MA, Uberbacher E, Hettich RL, et al. (2006) Detecting differential and correlated protein expression in label-free shotgun proteomics. J Proteome Res 5: 2909-2918.

15. Boyer RF (2001) Concepts in Biochemistry. 2nd edn, John Wiley & Sons, Inc, New York, USA.

16. Beagle B, Yang TL, Hung J, Cogger EA, Moriarty DJ, et al. (2005) The glycine N-methyltransferase (GNMT) 1289 C->T variant influences plasma total homocysteine concentrations in young women after restricting folate intake. J Nutr 135: 2780-2785.

17. Ferrando AA, Paddon-Jones D, Wolfe RR (2002) Alterations in protein metabolism during space flight and inactivity. Nutrition 18: 837-841.

18. Najjar SM, Yang Y, Fernström MA, Lee SJ, Deangelis AM, et al. (2005) Insulin acutely decreases hepatic fatty acid synthase activity. Cell Metab 2: 43-53.

19. Iwamoto J, Takeda T, Sato Y (2005) Interventions to prevent bone loss in astronauts during space flight. Keio J Med 54: 55-59.

20. Yamaguchi M (2005) Role of regucalcin in maintaining cell homeostasis and function (review). Int J Mol Med 15: 371-389.

21. Schmiedeknecht G, Büchler C, Schmitz G (1997) A bidirectional promoter connects the p14.5 gene to the gene for RNase P and RNase MRP protein subunit hPOP1. Biochem Biophys Res Commun 241: 59-67.